J|A|C|S ARTICLES

Published on Web 10/13/2009

Evaluation of Parameters Critical for Observing Nucleic Acids Inside Living *Xenopus laevis* Oocytes by In-Cell NMR Spectroscopy

Robert Hänsel,[†,‡] Silvie Foldynová-Trantírková,[§] Frank Löhr,[†,‡] Janina Buck,[‡,||] Eva Bongartz,[†,⊥] Ernst Bamberg,[†,⊥] Harald Schwalbe,[‡,||] Volker Dötsch,[*,†,‡] and Lukáš Trantírek[*,§,#]

Institute of Biophysical Chemistry, Goethe-University, Max-von-Laue Str. 9, 60438 Frankfurt am Main, Germany, Center for Biomolecular Magnetic Resonance and Cluster of Excellence Macromolecular Complexes, Goethe University, Max-von-Laue Strasse 9, 60438 Frankfurt am Main, Germany, Biology Centre of the AS CR, vvi and Faculty of Sciences, University of South Bohemia, Branišovská 31, 370 05 České Budějovice, Czech Republic, Institute for Organic Chemistry and Chemical Biology, Goethe-University, Max-von-Laue Str. 7, 60438 Frankfurt am Main, Germany, and Max-Planck-Institute of Biophysics, Department of Biophysical Chemistry, Max-von-Laue-Strasse 3, 60438 Frankfurt am Main, Germany

Received June 24, 2009; E-mail: vdoetsch@em.uni-frankfurt.de; trant@paru.cas.cz

Abstract: In-cell NMR spectroscopy of proteins in different cellular environments is a well-established technique that, however, has not been applied to nucleic acids so far. Here, we show that isotopically labeled DNA and RNA can be observed inside the eukaryotic environment of *Xenopus laevis* oocytes by in-cell NMR spectroscopy. One limiting factor for the observation of nucleic acids in *Xenopus* oocytes is their reduced stability. We demonstrate that chemical modification of DNA and RNA can protect them from degradation and can significantly enhance their lifetime. Finally, we show that the imino region of the NMR spectrum is devoid of any oocyte background signals enabling the detection even of isotopically nonlabeled molecules.

Introduction

It has been well established ever since the first experimental studies of the structure of nucleic acids (NA) that the cellular environment plays a significant role in determining the overall conformation, folding topology, and stability of NAs.[1−13] Conventional experimental techniques for structure determination such as X-ray crystallography and solution NMR spectroscopy, however, optimize sample conditions to either enhance crystal formation or properties improving NMR spectroscopy including spectral resolution and solubility rather than to mimic the physiological environment. This focus on the optimization of technical parameters neglects the effects of viscosity, molecular crowding and interaction with other macromolecules as well as the influence of the concentration of ions and other small molecules on the conformation and dynamics. Recent publications reporting the usage of *Xenopus laevis* (*X. laevis*) oocytes for eukaryotic in-cell NMR measurements of proteins[14−17] have in principle introduced the possibility of studying NAs directly in the eukaryotic environment. The stage IV *X. laevis* oocytes, which are arrested at the G2/M transition of the cell cycle, can be conveniently manipulated by microinjection, which

[†] Institute of Biophysical Chemistry, Goethe-University.
[‡] Center for Biomolecular Magnetic Resonance and Cluster of Excellence Macromolecular Complexes, Goethe University.
[§] University of South Bohemia.
[||] Institute for Organic Chemistry and Chemical Biology, Goethe-University.
[⊥] Max-Planck-Institute of Biophysics.
[#] Present address: Department of Chemistry, Utrecht University, Utrecht, The Netherlands.

(1) Brukner, I.; Susic, S.; Dlakic, M.; Savic, A.; Pongor, S. *J. Mol. Biol.* **1994**, *236*, 26–32.
(2) Chattopadhyaya, R.; Ikuta, S.; Grzeskowiak, K.; Dickerson, R. E. *Nature* **1988**, *334*, 175–19.
(3) Drew, H.; Takano, T.; Tanaka, S.; Itakura, K.; Dickerson, R. E. *Nature* **1980**, *286*, 567–573.
(4) Egli, M.; Williams, L. D.; Gao, Q.; Rich, A. *Biochemistry* **1991**, *30*, 11388–11402.
(5) Heddi, B.; Foloppe, N.; Hantz, E.; Hartmann, B. *J. Mol. Biol.* **2007**, *368*, 1403–1411.
(6) Hud, N. V.; Sklenar, V.; Feigon, J. *J. Mol. Biol.* **1999**, *286*, 651–660.
(7) Jerkovic, B.; Bolton, P. H. *Biochemistry* **2001**, *40*, 9406–9411.
(8) Kielkopf, C. L.; Ding, S.; Kuhn, P.; Rees, D. C. *J. Mol. Biol.* **2000**, *296*, 787–801.
(9) Kypr, J.; Chladkova, J.; Zimulova, M.; Vorlickova, M. *Nucleic Acids Res.* **1999**, *27*, 3466–3473.
(10) Mahendrasingam, A.; Rhodes, N. J.; Goodwin, D. C.; Nave, C.; Pigram, W. J.; Fuller, W.; Brahms, J.; Vergne, J. *Nature* **1983**, *301*, 535–537.
(11) Minasov, G.; Tereshko, V.; Egli, M. *J. Mol. Biol.* **1999**, *291*, 83–99.
(12) Noeske, J.; Schwalbe, H.; Wohnert, J. *Nucleic Acids Res.* **2007**, *35*, 5262–5273.
(13) Rhodes, N. J.; Mahendrasingam, A.; Pigram, W. J.; Fuller, W.; Brahms, J.; Vergne, J.; Warren, R. A. *Nature* **1982**, *296*, 267–269.
(14) Bodart, J. F.; Wieruszeski, J. M.; Amniai, L.; Leroy, A.; Landrieu, I.; Rousseau-Lescuyer, A.; Vilain, J. P.; Lippens, G. *J. Magn. Reson.* **2008**, *192*, 252–257.
(15) Sakai, T.; Tochio, H.; Tenno, T.; Ito, Y.; Kokubo, T.; Hiroaki, H.; Shirakawa, M. *J. Biomol. NMR* **2006**, *36*, 179–188.
(16) Selenko, P.; Serber, Z.; Gadea, B.; Ruderman, J.; Wagner, G. *Proc. Natl. Acad. Sci. U.S.A.* **2006**, *103*, 11904–11909.
(17) Serber, Z.; Selenko, P.; Hansel, R.; Reckel, S.; Löhr, F.; Ferrell, J. E., Jr.; Wagner, G.; Dötsch, V. *Nat. Protoc.* **2006**, *1*, 2701–2709.

permits the direct deposition of defined quantities of exogenous nucleic acid into the cellular environment. However, the adaptation of in-cell NMR to nucleic acids provides specific challenges. In-cell NMR experiments with overexpressed proteins as well as with proteins injected into oocytes have demonstrated that little to no background of oocyte signals is detected in [^{15}N,^{1}H]-HSQC spectra of ^{15}N-labeled proteins.[14−19] In-cell NMR experiments based on [^{13}C,^{1}H]-HSQC experiments, however, usually show a significant degree of such background or artifact signals necessitating the use of selective labeling[20] or special NMR filter techniques. In contrast to proteins, for which the [^{15}N,^{1}H]-HSQC is by far the most important experiment to monitor conformation and dynamics, ^{13}C-based NMR experiments provide an important source of information in the case of nucleic acids,[21] which increases the potential of problems with background signals. In addition, nucleic acids and in particular RNAs are quite sensitive to enzymatic degradation by nucleases. To investigate the potential for in-cell NMR experiments with nucleic acids, we have evaluated parameters critical for observing nucleic acids inside living *Xenopus laevis* oocytes. Here we demonstrate that in-cell NMR with DNA and RNA is feasible in this eukaryotic system and can be used for the investigation of structure and stability of nucleic acids (DNA and RNA) under physiological conditions. In addition, we demonstrate that monitoring secondary structure and folding topology of nucleic acids in *Xenopus* oocytes using in-cell NMR can be achieved even without isotopically labeled samples.

Experimental Section

Sample Preparation and (In-Cell) NMR Spectroscopy. The uniformly labeled (^{13}C and ^{15}N) d(GCGAAGC) and r(GGCACUUCGGUGCC) hairpins were purchased from Silantes GmbH (München, Germany). Unlabeled samples comprising unmodified d(GCGAAGC) and r(GGCACUUCGGUGCC) hairpins and $dG_3(TTAG_3)_3T$ G-quadruplex, phosphothioate modified d(GCGAAGC) and r(GGCACUUCGGUGCC) hairpins, and O2′-hydroxyl methylated r(GGCACUUCGGUGCC) were purchased from Microsynth (Switzerland) and/or Generi-Biotech (Czech Republic). The in vitro NMR experiments with DNA and RNA hairpins were performed in 25 mM HEPES buffer (pH = 7.5), 50 mM NaCl, and 1 mM DTT, whereas experiments with $dG_3(TTAG_3)_3T$ were carried out in a buffer mimicking the intraoocyte environment (25 mM HEPES (pH = 7.5), 10.5 mM NaCl, 110 mM KCl, 130 nM $CaCl_2$, 1 mM $MgCl_2$, 10% D_2O;[22] named intraoocyte buffer in the remainder of this manuscript). In-cell NMR samples were prepared by injecting a 50 nL aliquot of the stock solution (5 mM (250 μM intracellular concentration) [u-^{13}C,^{15}N] DNA or RNA, 25 mM HEPES (pH = 7.5), 50 mM NaCl, and 1 mM DTT) into each oocyte. A 10 mM stock solution of DNA or RNA hairpin was used for injections of isotopically unlabeled NA samples, resulting in an intracellular concentration of 500 μM. In-cell samples of $dG_3(TTAG_3)_3T$ were prepared from a stock solution of 1.2 mM (60 μM intracellular concentration). Higher intracellular concentrations of quadruplex DNA than 250 μM resulted in the induction of cell death. To verify oocyte integrity, 10 out of 200 injected oocytes were maturated to eggs by addition of 1 μM progesterone (data not shown).

The NAs prepared enzymatically were injected directly. The samples obtained from chemical synthesis were subjected to butanol precipitation prior to injection. For butanol precipitation, lyophillized NA was dissolved in 200 μL of H_2O and mixed together with 15 mL of n-butanol. The mixture was vigorously vortexed for 10 min at room temperature. Precipitated NA was removed by centrifugation at 30 000 g for 45 min. For injection, the precipitated NA was dissolved in injection buffer and reannealed by heating the NA sample to 95 °C for 10 min and then letting the sample slowly cool down to room temperature. After injection, the oocytes were transferred to a Petri dish, washed thoroughly with excess volumes of Ori-Ca^{2+} buffer (5 mM HEPES (pH = 7.6), 110 mM NaCl, 5 mM KCl, 2 mM $CaCl_2$, and 1 mM $MgCl_2$) and allowed to recover for 1 h. Roughly 200 oocytes were injected over a period of approximately three hours. The injected oocytes were collected and transferred to a Shigemi tube (without the plunger) and kept in a total volume of 1 mL of Ori buffer containing 10% of D_2O. Every 5 h the external buffer was exchanged and investigated by NMR for the detection of NA. Samples for measurements in cleared lysate were prepared as follows: after the in-cell NMR measurements, oocytes were transferred into a Petri dish prefilled with Ori-Ca^{2+} buffer. Subsequently the Petri dish was transferred into an ice-box and cooled down for 15 min. Oocytes were transferred into another Petri dish prefilled with 10 mL ice cold buffer mimicking the oocyte salt environment. Afterward oocytes were transferred into an eppendorf tube and the final volume was adjusted to 500 μL with buffer. The oocytes were mechanically crushed and insoluble fractions were removed by centrifugation at 20 000 g for 20 min. The supernatant was transferred into an eppendorf tube and heated to 95 °C for 10 min. Precipitated proteins were removed by centrifugation at 20 000 *g* for 10 min. The supernatant (250 μL) was used for NMR measurements.

NMR experiments were performed using Bruker Avance 700 and 600 MHz spectrometer equipped with cryogenic triple-resonance probes at a sample temperature of 18 °C. The imino groups were observed using [^{15}N−^{1}H]-SOFAST-HMQC experiments[23] with the ^{15}N carrier frequency set to 150 ppm and the ^{1}H excitation maximum set to 12.8 ppm. For detection of the amino groups, the ^{15}N carrier frequency and the ^{1}H excitation maximum were changed to 96 ppm and 8 ppm, respectively. The ribose and cytosine C5 proton-carbon correlation spectra were obtained using an HSQC sequence, which employs gradient coherence selection but no sensitivity enhancement. The ^{13}C carrier was positioned at 62 ppm. The remaining nucleobase ^{1}H and ^{13}C signals were observed in constant-time [^{13}C−^{1}H]-CT-TROSY experiments[24] with the ^{13}C carrier set to 147 ppm. The total delay with ^{13}C transverse magnetization was set to a fixed value of 14.2 ms. In addition, the nitrogen nuclei were decoupled during the ^{13}C evolution time. The 1D ^{1}H spectra were recorded using a 11-echo pulse sequence[25] with the excitation maximum adjusted to the center of the imino region (ca. 12.8 ppm).

Fluorimetric Leakage Essay. The time-course of leakage of d(GCGAAGC) from injected *X. laevis* oocytes was assayed by measuring the fluorescence intensity of the buffer surrounding the injected oocytes relative to the fluorescence intensity of a reference sample. Two different samples were prepared by injecting 50 nL of a 5 mM stock solution of the 5′-fluoresceine tagged d(GCGAAGC) into each of 55 oocytes. After injection, the oocytes were washed with fresh Ori buffer and allowed to recover for 1 h. Subsequently, the injected oocytes were washed with fresh Ori buffer and transferred into a cuvette (10 mm light path). In one sample, the buffer was not exchanged and the increase in the fluorescence signal in the buffer above the oocytes was measured approximately every hour. In contrast, the buffer in the second sample was exchanged and the oocytes were washed following

(18) Serber, Z.; Keatinge-Clay, A. T.; Ledwidge, R.; Kelly, A. E.; Miller, S. M.; Dötsch, V. *J. Am. Chem. Soc.* **2001**, *123*, 2446–2447.
(19) Serber, Z.; Ledwidge, R.; Miller, S. M.; Dötsch, V. *J. Am. Chem. Soc.* **2001**, *123*, 8895–8901.
(20) Serber, Z.; Straub, W.; Corsini, L.; Nomura, A. M.; Shimba, N.; Craik, C. S.; Ortiz de Montellano, P.; Dötsch, V. *J. Am. Chem. Soc.* **2004**, *126*, 7119–7125.
(21) Fürtig, B.; Richter, C.; Wöhnert, J.; Schwalbe, H. *Chembiochem* **2003**, *4*, 936–962.
(22) Weber, W. M. *Biochim. Biophys. Acta* **1999**, *1421*, 213–233.
(23) Schanda, P.; Brutscher, B. *J. Am. Chem. Soc.* **2005**, *127*, 8014–8015.
(24) Pervushin, K.; Riek, R.; Wider, G.; Wuthrich, K. *J. Am. Chem. Soc.* **1998**, *120*, 6394–6400.
(25) Sklenar, V.; Bax, A. *J. Magn. Reson.* **1987**, *74*, 469–479.

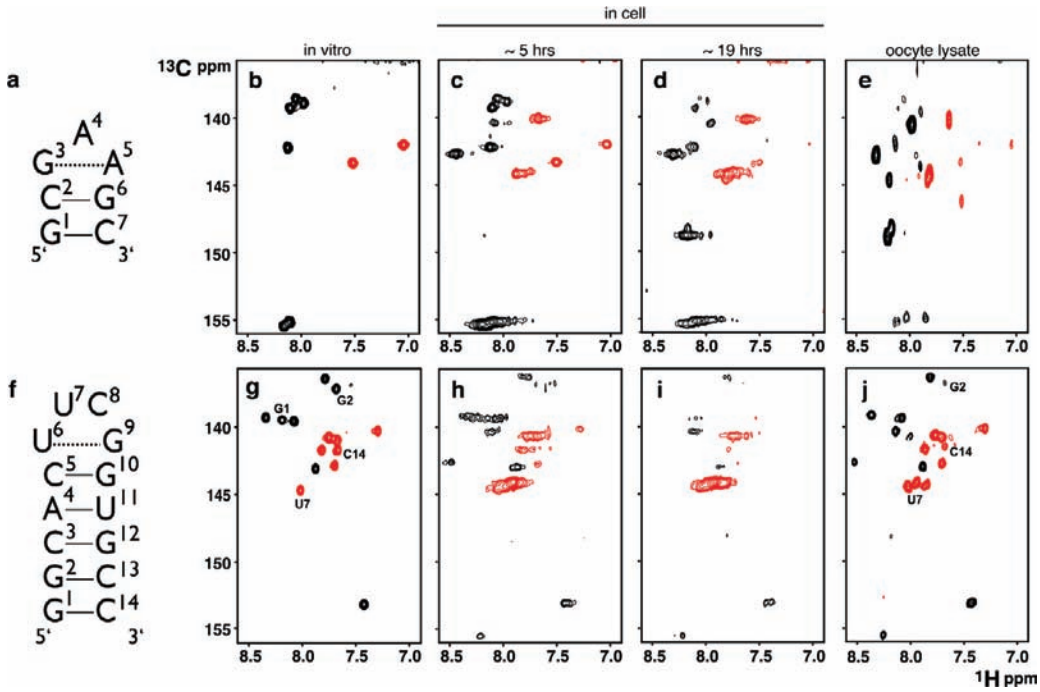

Figure 1. (b−e) and (g−j) \Aromatic regions of the 2D [^{1}H−^{13}C]-CT-TROSY-HSQC spectra of ^{13}C/^{15}N-labeled d(GCGAAGC) and r(GGCACUUCGGUGCC) hairpins. (a) and (f) Schematic representations of secondary structures for d(GCGAAGC) and r(GGCACUUCGGUGCC), respectively. (b) and (g) In vitro spectra of d(GCGAAGC) and r(GGCACUUCGGUGCC). (c) and (d) In-cell NMR spectra of d(GCGAAGC) recorded approximately 5 and 19 h after microinjection of the *X. laevis* oocytes. (h) and (i) Analogous spectra to (c) and (d) for the r(GGCACUUCGGUGCC) molecule. (e) and (j) In vitro spectra of d(GCGAAGC) and r(GGCACUUCGGUGCC) in cleared oocyte lysates. The signals in black (positive) and red (negative) correspond to purines and to pyrimidines, respectively. The difference in sign of the purine and the pyrimidine peaks is due to the constant-time mode of the experiment.

measurement of the fluorescence at 2.5, 5, and 10 h. For preparation of the reference sample, 55 injected oocytes were recovered, lysed, and proteins were removed by thermal denaturation. The fluorescence of this sample was set to 100% and used to calculate the percentage of DNA that leaked out of the oocytes in the other two samples. The fluorescence intensities were measured at 520 nm that corresponds to the emission maximum of fluoresceine.

Results

To evaluate the potential to use in-cell NMR for the investigation of nucleic acids we injected double labeled (^{13}C and ^{15}N) d(GCGAAGC) DNA and r(GGCACUUCGGUGCC) RNA hairpins into *X. laevis* oocytes and subsequently acquired a series of 1D and 2D NMR spectra. Figure 1 shows the comparisons of in vitro and in-cell NMR spectra of the aromatic region of the nucleic acid constructs recorded as a function of time. Spectra taken five hours after injection show the basic pattern of the NAs seen in the in vitro samples. The line width of the signals of the in-cell spectra, however, is significantly increased which is partially due to the higher viscosity of the cellular environment and the reduced homogeneity of the oocyte sample as compared to the less viscous and more homogeneous in vitro conditions. Although the spectral patterns for the aromatic signals corresponding to both the DNA and the RNA hairpin structures appear to be essentially identical to those observed in vitro, their intensities decreased over time (Figures 1c, 1d, 1h, and 1i). In parallel with this decrease in the signal intensities, new signals appeared. These additional peaks may arise either due to NA degradation, conformational changes, or the interaction of the injected NA with cellular components. Analysis of mass-spectroscopy data using 5′- and 3′-biotin-tagged NA samples injected into *X. laevis* oocytes revealed that the DNA substrate d(GCGAAGC) was degraded to mononucleotides. The MS data also indicated that degradation of this substrate proceeded in two steps. In the first step, the DNA was cleaved at G1p and at C2p indicating cleavage by an exonuclease and endonuclease (data not shown). In the second step, the disrupted DNA hairpin was degraded to mononucleotides as indicated by chemical shift values that corresponded to free nucleotides. After 24 h, the oocytes were lysed and the proteins were removed by thermal denaturation. The NMR spectral pattern in the cleared lysate (Figure 1e) was similar to that observed for the in-cell sample after 19 h postinjection (Figure 1d). As a final proof to refute the possibility that the new signals were due to a conformational change, we extracted cleared oocyte lysate with n-butanol. While the DNA hairpin is precipitated by n-butanol, small molecules like mononucleotides dissolve in it. The NMR spectrum of the lyophilized butanol fraction showed a spectral pattern corresponding exclusively to the newly appeared signals in in-cell spectra after 19 h postinjection (data not shown) suggesting that the DNA is degraded.

Similarly to the DNA hairpin, the aromatic resonances of the injected RNA broadened and most of them virtually diminished over time with the exception of the resonances of U6 and U7 that are located in the flexible loop region[26,27] (Figure 1h and i). This disappearance of the signals without the appearance of additional peaks with chemical shifts of the isolated nucleotides suggested that the RNA hairpin is not completely degraded but rather interacts with cellular components leading to slower rotational tumbling and concomitant line broadening and disappearance of peaks. To further investigate this interpretation, the oocytes containing the injected RNA were lysed and the proteins were removed by thermal denaturation. The precipitated

(26) Duchardt, E.; Schwalbe, H. *J. Biomol. NMR.* **2005**, *32*, 295–308.
(27) Ferner, J.; Villa, A.; Duchardt, E.; Widjajakusuma, E.; Wöhnert, J.; Stock, G.; Schwalbe, H. *Nucleic Acids Res.* **2008**, *36*, 1928–1940.

proteins and insoluble fractions of the cells were then removed by centrifugation. The NMR spectrum of the cleared lysate showed most of the resonances of the in vitro spectrum of the RNA, suggesting that the RNA does not get cleaved to the level of single nucleotides (Figure 1j). This observation supported the idea that the disappearance of the resonances of the RNA in the in-cell spectra was due to RNA interaction with large cellular components. To further investigate the state of the RNA, the cleared lysate was butanol precipitated. The NMR spectrum of the lyophilized butanol fraction indicated the presence of free cytidine and guanosine nucleotides (Supplementary Figure 1a, Supporting Information) while the spectrum of the resolubilized precipitate showed a mixture of the original peaks and peaks that correspond to an RNA hairpin without G1 and C14 (Supplementary Figure 1b and c, Supporting Information). Analysis by mass spectrometry using 5′-biotin tagged RNA incubated within *X. laevis* oocytes revealed partial RNA degradation involving cleavage of the terminal C14. In combination, the NMR and MS data indicate that both C14 and G1 are cleaved but the remaining RNA molecule was not further degraded. The reason that the MS data only showed cleavage of C14 but not of G1 is the protection of the 5′-end by the biotin tag that was attached to the RNA used for MS analysis. In the NMR samples that did not have a biotin-tag, G1 was completely lost and the signal intensity of C14 was notably reduced (Supplementary Figure 1b, Supporting Information).

Chemical Modifications of the Backbone Stabilize NAs. To investigate whether the DNA could potentially be stabilized against degradation, a modified d(GCGAAGC) DNA substrate, with the first and second phosphate groups replaced by phosphorothioate groups, was injected into *X. laevis* oocytes or added to *X. laevis* oocytes lysate. The NMR measurements revealed that the phosphorothioate modified DNA was resistant to nuclease cleavage in contrast to the unmodified DNA. (Supplementary Figure S2, Supporting Information). Surprisingly, modification of the first phosphate group alone did not protect the DNA from degradation but resulted in a slowdown of the reaction.

RNA molecules are generally considered more susceptible to enzymatic degradation than DNA. Surprisingly, our measurements indicated that the RNA used in this study was more resistant toward degradation than the DNA hairpin. In analogy to the DNA, we tested the possibility to stabilize RNA against degradation via phosphorothioate modification of the backbone and in addition by methylation of the O2′-hydroxyl groups of the RNA. Both chemical modifications were able to stabilize the RNA against degradation (data not shown).

Noteworthy, phosphorothioate modification of the NA backbone as well as methylation of RNA O2′-hydroxyl groups are today routinely available at almost no extra costs as compared to unlabeled and unmodified samples. In addition, replacement of the oxygen atom(s) in the phosphodiester group by sulfur leads to a dramatic change in the chemical shift of the affected phosphorus by about 50 ppm. Due to this shift, the phosphorothioate modified NA can be easily monitored via ^{31}P NMR spectroscopy inside living cells, as there is no interference from the oocyte background (Supplementary Figure 3, Supporting Information). However, when considering ^{31}P NMR measurements on phosphorothioate-modified sample, one has to keep in mind that standard phosphorothioate modified DNA/RNA are prepared from racemic precursors. Consequently, the single ^{31}P signal of the original phosphate group splits into up to three different signals when replaced with a phosphorothioate group. Two of these signals represent the pro-(S) and pro-(R) phosphorothioates while the third signal is due to the presence of phosphoro-dithioate, an artifact of the synthesis.

Available Experimental Time-Window for In-Cell NMR Experiments. In general, the available time-window for in-cell NMR measurements is dictated by the stability of NAs from degradation, the life span of *X. laevis* oocytes, and the leakage of small NA constructs out of the cells via incisions made during injection, for example. The signal pattern corresponding to the original DNA and RNA hairpins could be observed for at least 6 to 7 h postinjection, even in the absence of stabilizing backbone modifications. As demonstrated by Sakai et al., if properly treated the *X. laevis* oocytes live for a period of at least 20 h after injection.[15] In that respect, the life span of both NAs and the oocytes did not represent a key limitation for monitoring of NAs in the cellular environment. On the other hand, leakage of proteins[28] or NAs out of the oocytes can occur on much shorter time scales. In order to estimate the time restrictions due to leakage of NA from the injected oocytes, we performed a fluorimetric assay. These data indicated that when the buffer was exchanged between individual NMR experiments every four to five hours, the amount of leaked NA from the oocytes was less than 5% (Supporting Information Figure S4). Such an amount of leaked NA is expected to not interfere with the in-cell NMR measurements.

Evaluation of Oocyte Background Interference with Signals from NA. As shown above, the background from oocyte signals does not pose a problem for the detection of NA resonances in the aromatic region. Comparison of in-cell spectra with in vitro spectra of NAs revealed that isotopic labeling results in unambiguous identification of imino and amino signals of the injected nucleic acids as well (Figure 2d, e, and f). In these spectral regions as well as the aromatic region, virtually no background signals exist. In contrast, spectra of the aliphatic/sugar regions containing the C2′−H2′/H2″and C5′−H5′/H5″ cross peaks show significant background from the oocytes (Figure 2a and c) while the C3′−H3′ region of the 2D ^{1}H−^{13}C HSQC spectrum is dominated by a strong artifact resulting from the suppressed water signal. Finally, essentially no background from oocyte signals is seen in the C1′−H1′ and C4′−H4′ regions and signals from isotopically labeled NA can be easily identified (Figure 2b).

Unlabeled NA Can Be Observed in the Cellular Environment. One of the practical limitations of the applications of in-cell NMR to the investigation of biomolecules in the cellular environment is the requirement to label the samples, which makes the in-cell NMR experiments on NA costly. However, the ^{1}H background signals from the oocytes are significantly less in some spectral regions than in others, thus potentially enabling the observation of specific resonances of unlabeled NAs. Figure 3a shows a ^{1}H NMR spectrum of *X. laevis* oocytes that exhibited strong ^{1}H background signals in the aromatic and the amino regions. Selective detection of NA resonances in these regions would require isotopical labeling. In contrast, the imino region did not possess any oocyte signals. In order to test the possibility of monitoring the imino resonances of unlabeled NA species within the cellular environment, we injected the oocytes with both unlabeled DNA and RNA hairpins. The spectra shown in Figure 3d and e demon-

(28) Sakai, T.; Tochio, H.; Inomata, K.; Sasaki, Y.; Tenno, T.; Tanaka, T.; Kokubo, T.; Hiroaki, H.; Shirakawa, M. *Anal. Biochem.* **2007**, *371*, 247–249.

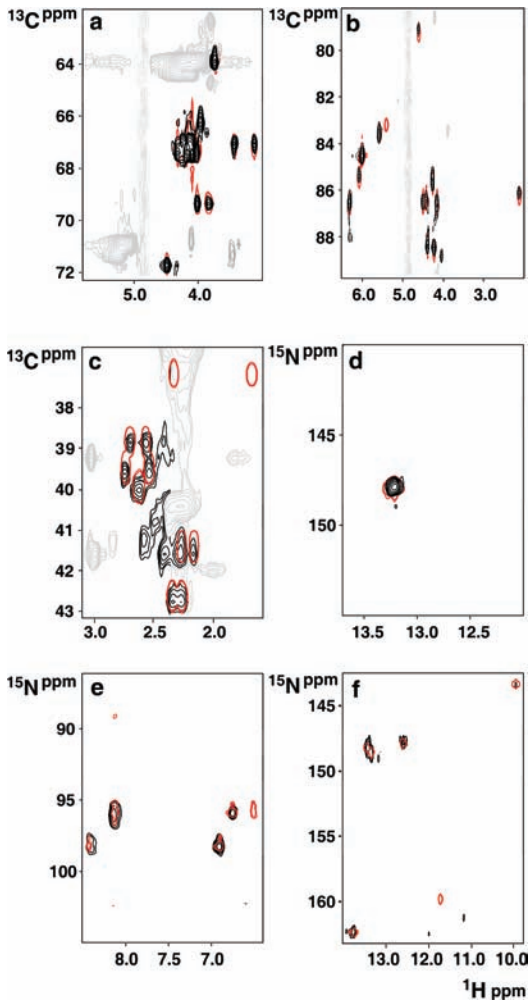

Figure 2. Interference of the *Xenopus laevis* spectral background with signals from exogenous NA. The selected regions show the in-cell 2D [^{1}H−^{13}C]-CT-TROSY-HSQC (a, b, and c) and the [^{1}H−^{15}N]-SOFAST-HMQC spectra (d and e) of the ^{13}C and ^{15}N-labeled d(GCGAAGC). (f) Imino region of the [^{1}H−^{15}N]-SOFAST-HMQC spectrum of the ^{13}C and ^{15}N-labeled r(GGCACUUCGGUGCC). The signals in black and red correspond to in-cell and to the reference in vitro spectra of d(GCGAAGC) and r(GGCACUUCGGUGCC), respectively. Of the red signals, only the first contour level is shown.

strate that the chemical shifts of the imino protons of unlabeled NAs, which are indicators of base-pairing among the bases and folding topology, can be monitored using 1D ^{1}H in-cell NMR experiments.

We observed that injection of synthetically prepared NA samples was lethal to the oocytes. It appeared that synthetically prepared samples of nucleic acids contained some low-molecular weight impurities, which at concentration used for the injection were toxic to the oocytes. To allow for injection of synthetically prepared NAs, the NAs needed to be butanol precipitated prior to injection. One butanol precipitation cycle was typically enough to remove toxic contaminants from the NA sample. The precipitated nucleic acid samples dissolved in injection buffer and subsequently reannealed could be injected into oocytes subsequently without any harm.

While these data show that unlabeled NA samples can in principle be used to obtain at least some information about the conformation of the macromolecule the use of labeled samples offers many advantages such as the ability to suppress oocyte background signals in regions other than that of the imino protons. However, these advantages of labeled samples are counter-balanced by the relatively high sample costs. In contrast to protein samples, labeled NAs can be recovered to a large extent after the in-cell NMR experiments (assuming that the sample does not get degraded). For recovery of the sample, the oocytes are mechanically crushed and subsequently heated to 95 degrees for 10−15 min to precipitate all proteins. The NAs can be obtained from the supernatant by butanol extraction and after resolubilization and reannealing the NA can be reused for other measurements. The recovery yield was 70% in the case of the RNA hairpin.

Application of In-Cell NMR to Investigate the Intracellular Behavior of Vertebrate Telomeric Repeat DNA. One class of DNA structures that has been in the focus of structural biology for a long time are G-quadruplexes.[29−39] These four-stranded helical structures form at the 3′ end of chromosomes of vertebrates where thousands of tandem repeats of the G-rich sequence $(GGGTTA)_n$ constitute the telomers.[40] It has been demonstrated that formation of such quadruplex structure by telomeric DNA inhibits the activity of telomerase,[41] an enzyme that is critical for proliferation of most cancer cells.[42] On the basis of these findings, the stabilization of telomeric G-quadruplexes by ligands is expected to be a new promising strategy for development of anticancer drugs.[43,44] Previous studies on various four-repeat human telomeric G-rich sequences have revealed a diverse range of intramolecular G-quadruplex structures under different experimental conditions.[38,45−51] The G-quadruplex topology has been shown to depend on the nature of the counterion, on molecular crowding effects and on sequence composition, for example. Although, the structural behavior of telomeric repeats has been investigated in great

(29) Gatto, B.; Palumbo, M.; Sissi, C. *Curr. Med. Chem.* **2009**, *16*, 1248–1265.
(30) Huppert, J. L. *Chem. Soc. Rev.* **2008**, *37*, 1375–1384.
(31) Huppert, J. L. *Biochimie* **2008**, *90*, 1140–1148.
(32) Huppert, J. L.; Balasubramanian, S. *Nucleic Acids Res.* **2005**, *33*, 2908–2916.
(33) Huppert, J. L.; Balasubramanian, S. *Nucleic Acids Res.* **2007**, *35*, 406–413.
(34) Lipps, H. J.; Rhodes, D. *Trends Cell Biol.* **2009**, *19*, 414–422.
(35) Neidle, S.; Parkinson, G. N. *Biochimie* **2008**, *90*, 1184–1196.
(36) Ou, T. M.; Lu, Y. J.; Tan, J. H.; Huang, Z. S.; Wong, K. Y.; Gu, L. Q. *ChemMedChem* **2008**, *3*, 690–713.
(37) Phan, A. T.; Kuryavyi, V.; Patel, D. J. *Curr. Opin. Struct. Biol.* **2006**, *16*, 288–298.
(38) Qin, Y.; Hurley, L. H. *Biochimie* **2008**, *90*, 1149–1171.
(39) Wong, H. M.; Payet, L.; Huppert, J. L. *Curr. Opin. Mol. Ther.* **2009**, *11*, 146–155.
(40) Makarov, V. L.; Hirose, Y.; Langmore, J. P. *Cell* **1997**, *88*, 657–666.
(41) Zahler, A. M.; Williamson, J. R.; Cech, T. R.; Prescott, D. M. *Nature* **1991**, *350*, 718–720.
(42) Kim, N. W.; Piatyszek, M. A.; Prowse, K. R.; Harley, C. B.; West, M. D.; Ho, P. L.; Coviello, G. M.; Wright, W. E.; Weinrich, S. L.; Shay, J. W. *Science* **1994**, *266*, 2011–2015.
(43) Mergny, J. L.; Helene, C. *Nat. Med.* **1998**, *4*, 1366–1367.
(44) Sun, D.; Thompson, B.; Cathers, B. E.; Salazar, M.; Kerwin, S. M.; Trent, J. O.; Jenkins, T. C.; Neidle, S.; Hurley, L. H. *J. Med. Chem.* **1997**, *40*, 2113–2116.
(45) Dai, J.; Carver, M.; Yang, D. *Biochimie* **2008**, *90*, 1172–1183.
(46) Inoue, M.; Miyoshi, D.; Sugimoto, N. *Nucleic Acids Symp. Ser. (Oxf)* **2005**, 243–244.
(47) Kypr, J.; Kejnovska, I.; Renciuk, D.; Vorlickova, M. *Nucleic Acids Res.* **2009**, *37*, 1713–1725.
(48) Miyoshi, D.; Matsumura, S.; Li, W.; Sugimoto, N. *Nucleosides Nucleotides Nucleic Acids* **2003**, *22*, 203–221.
(49) Miyoshi, D.; Nakao, A.; Sugimoto, N. *Nucleic Acids Res. Suppl.* **2001**, 259–260.
(50) Miyoshi, D.; Nakao, A.; Sugimoto, N. *Biochemistry* **2002**, *41*, 15017–15024.
(51) Miyoshi, D.; Nakao, A.; Sugimoto, N. *Nucleic Acids Res.* **2003**, *31*, 1156–1163.

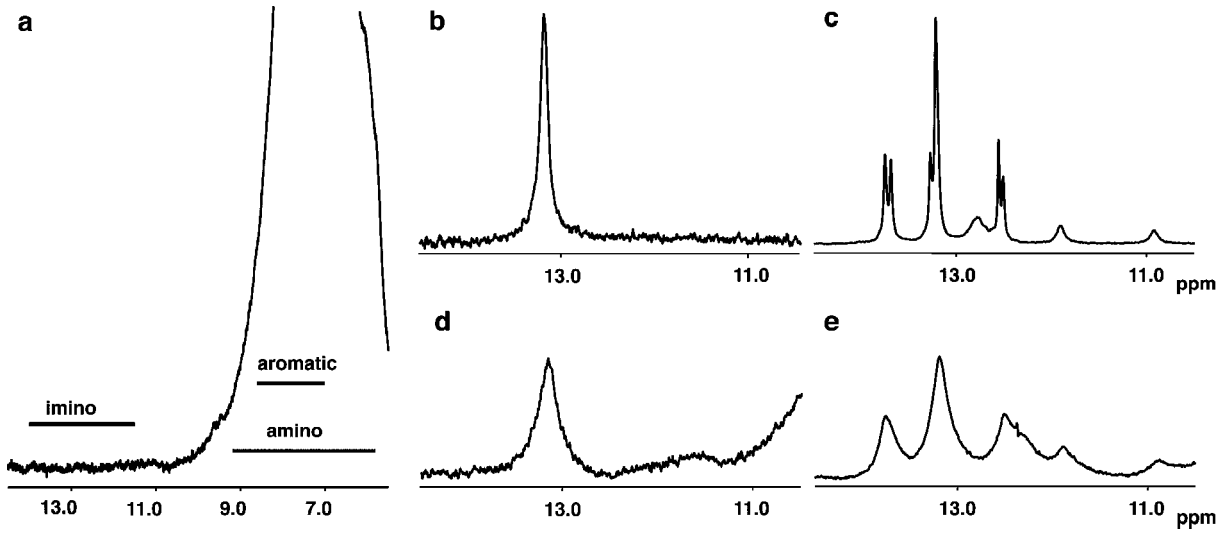

Figure 3. Imino regions of the 1D ^{1}H 11-echo spectra of *X. laevis* oocytes (a), the spectra of the phosphorothioate modified DNA d(G*C*GAAGC) ((b) and d)), and the spectra of the O2′-methylated RNA r(GGCACUUCGGUGCC) ((c) and (e)). (d) and (e) In-cell NMR spectra. (b) and (c) In vitro NMR spectra of d(G*C*GAAGC) and O2′-methylated r(GGCACUUCGGUGCC), respectively.

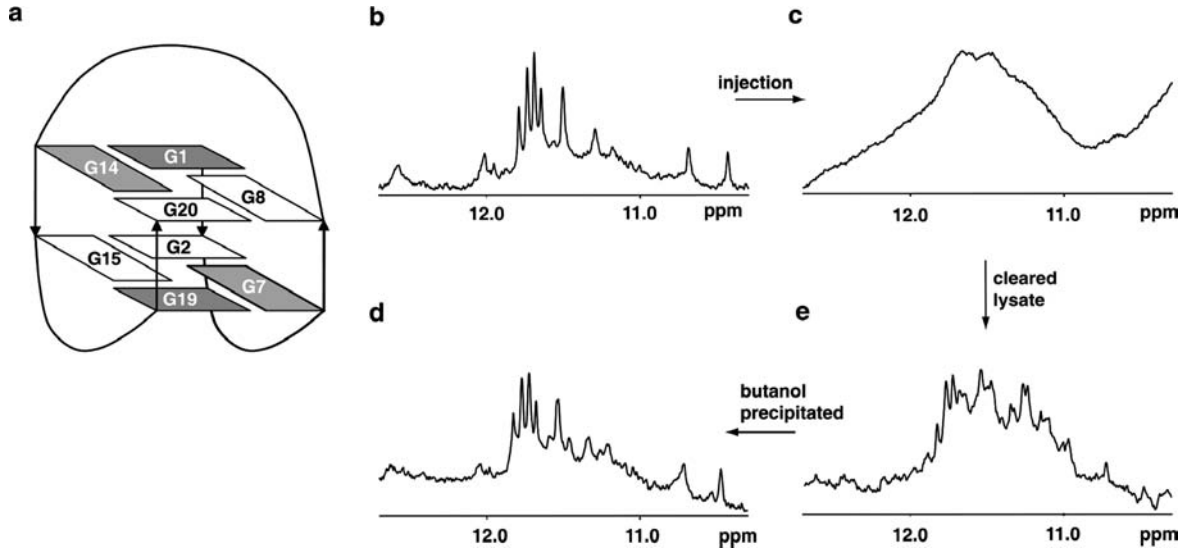

Figure 4. (a) Schematic representation of the structure of the human telomeric repeat DNA fragment d($G_3(TTAG_3)_3T$) according to Lim et al.[53] *Anti* and *syn* guanines are colored in gray and white, respectively.(b), (c), and (e) Imino regions of the 1D ^{1}H 11-echo spectra of the d($G_3(TTAG_3)_3T$) in intraoocyte buffer (in vitro), in *X. laevis* oocytes (in-cell), and in cleared lysate, respectively. (d) Imino region of 1D ^{1}H 11-echo spectrum of d($G_3(TTAG_3)_3T$) butanol precipitated from a cleared lysate and reannealed in intraoocyte buffer.

detail in vitro revealing their considerable conformational heterogeneity, the biologically relevant in vivo G-quadruplex topology remains unknown. To obtain first insights into possible conformations of G-quadruplexes in the cellular environment, we have injected an unlabeled d($G_3(TTAG_3)_3T$) fragment into *X. laevis* oocytes. This particular sequence was recently shown to adopt a stable basket-type G-quadruplex in potassium ion containing solutions.[52] The in vitro 1D spectrum shows the expected signal pattern for a basket-type G-quadruplex[52] (Figure 4b). In contrast, the imino region of the in-cell NMR spectrum is dominated by a single, broad peak with two apparent maxima centered at 11.5 and 11.7 ppm (Figure 4c). While the low resolution of the in-cell spectrum does not allow for a direct structural interpretation of the spectrum, its difference to the in vitro spectrum suggests that conformational differences between the in vitro condition and the in-cell condition exist.

It has been demonstrated that oocyte lysates preserve many features of the intact cell and can be good substitutes for the oocytes themselves (cf. Figure 1). For NMR spectroscopy mixing labeled macromolecules with oocyte lysate has the major advantage that the improved homogeneity of the sample significantly reduces the line width of the spectra. To further investigate the state of the telomeric DNA under native-like conditions we crushed the injected oocytes, removed most proteins by thermal denaturation and recorded ^{1}H 1D spectra in these cleared *X. laevis* oocyte lysate (Figure 4e). If changes in the conformation of the DNA can be detected these changes are most likely due to interaction with the remaining components

(52) Lim, K. W.; Amrane, S.; Bouaziz, S.; Xu, W.; Mu, Y.; Patel, D. J.; Luu, K. N.; Phan, A. T. *J. Am. Chem. Soc.* **2009**, *131*, 4301–4309.

(53) Cornish, P. V.; Giedroc, D. P.; Hennig, M. *J. Biomol. NMR* **2006**, *35*, 209–223.

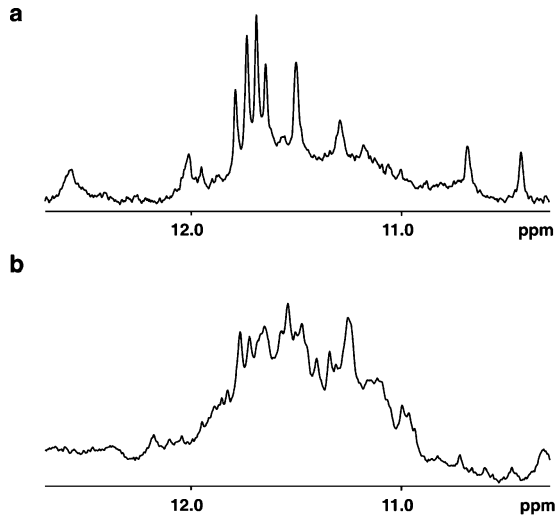

Figure 5. Imino regions of the 1D ^{1}H 11-echo spectra of the $d(G_3(TTAG_3)_3T)$ in intraoocyte buffer (a) and in cleared lysate (b).

of the cleared lysate, small molecules and ions. The imino signal pattern of the spectrum measured in cleared lysate is quite different from the typical basket-type G-quadruplex suggesting that substantial conformational differences exist between the states observed in vitro and in the cleared lysate. To investigate whether the observed differences were due to DNA degradation, we recovered the DNA from the cleared lysate by butanol precipitation and redissolved and annealed it in intraoocyte buffer. Virtually identical patterns of the original in vitro spectrum and of the spectrum of the DNA recovered from injected oocytes/cleared lysate demonstrated that the DNA was not degraded within the oocytes or lysate (Figure 4d). Mixing or annealing the DNA directly with the cleared lysate showed virtually the same peak pattern as the DNA in the cleared lysate that was produced by crushing injected oocytes, showing that the new conformation or mixture of conformations can be directly investigated in cleared oocyte lysate (Figure 5).

Interestingly, the overall shape of the signal pattern of the imino region measured in cleared lysate resembles the shape of the imino region measured with the G-DNA injected into oocytes (Supporting Information Figure S5, S6). While further analysis of the conformation or the mixture of conformations observed in the oocytes/cleared lysate will have to be based on a detailed structure determination of the telomeric DNA in cleared lysate, these data already demonstrate that in-cell NMR spectroscopy with unlabeled NAs can provide interesting insight into conformations that are adopted in the cellular environment.

Discussion

The goal of in-cell NMR spectroscopy is to provide information about the conformation, dynamics and intermolecular interactions of biological macromolecules with their cellular environment in a setting that mimics their natural surrounding as much as possible.[18] Here we have demonstrated that both DNA as well as RNA hairpins and DNA quadruplexes can be observed when injected into *X.laevis* oocytes by in-cell NMR, the main limitation being the degradation of the molecules. DNA and RNA can, however, be stabilized against degradation by chemical modifications that are easily introduced by standard chemistry during the chemical synthesis of these molecules. The use of chemically modified NA, however, should be considered with caution. There are several indications that introduction of phosphorothioate groups and in particular methylation of the RNA O2′-hydroxyl groups can influence the conformation of the NA.[53−61] In RNA, the O2′-hydrogen is involved in hydrogen bonding and constitutes one of the main sources of RNA stabilization and structure forming factors. In that respect, the methylation of O2′-hydroxyls may disrupt natural hydrogen bonding pattern and might destabilize or change the RNA conformation.

In two out of three cases presented in this investigation, degradation occurred. In both cases, the degradation sites were located at the terminal base-pairs. For structural investigations of nucleotides situated in loops, the use of minimally, directly at the degradation sites modified DNA/RNA could be a good alternative that does not affect the loop conformation. For each NA however this assumption should be tested in vitro. It should also be mentioned that before injection of expensive NA samples, the susceptibility to degradation can be tested with much cheaper unlabeled NA samples. If degradation is a problem, analysis of degradation pattern, for example, via MS analysis of biotin tagged NA, represents a very efficient way to design minimally modified constructs suitable for in-cell NMR measurements.

Nonetheless, the best strategy for diminishing the effect of degradation is shortening of the injection time and duration of the measurement. Manual injection of NA takes between three to four hours depending on experience of the person performing the injection. The use of robotic injection devices shortens the injection time to about four minutes thus enabling acquisition of the NMR spectra within 2 h post injection[17,62] (after injection a resting period of 1 h is necessary to close the incision). As far as reduction of measurement time is concerned, nonlinear sampling and projection reconstruction techniques have recently been used to significantly shorten the time of the experiment[63,64] and has allowed for the complete structure determination of a protein inside living *E. coli* cells. Such experimental set ups could also be employed for more detailed structural investigations of NAs in oocytes.

For the investigation of the influence of factors such as general molecular crowding or ionic composition, cellular lysates represent a good alternative since they provide in general a significantly higher homogeneity and much improved line width[16,17] as demonstrated with the quadruplex experiments. Interestingly, cellular extracts from *Xenopus* oocytes can be produced in a cell-cycle competent form in which many cellular

(54) Fohrer, J.; Hennig, M.; Carlomagno, T. *J. Mol. Biol.* **2006**, *356*, 280–287.
(55) Jucker, F. M.; Heus, H. A.; Yip, P. F.; Moors, E. H.; Pardi, A. *J. Mol. Biol.* **1996**, *264*, 968–980.
(56) Kanzaki, T.; Nakano, S.; Sugimoto, N. *Nucl. Acids Res. Suppl.* **2002**, 189–190.
(57) Liu, J.; Lilley, D. M. *RNA* **2007**, *13*, 200–210.
(58) Sponer, J. E.; Spackova, N.; Kulhanek, P.; Leszczynski, J.; Sponer, J. *J. Phys. Chem. A* **2005**, *109*, 2292–2301.
(59) Sponer, J. E.; Spackova, N.; Leszczynski, J.; Sponer, J. *J. Phys. Chem. B* **2005**, *109*, 11399–11410.
(60) Wang, S.; Kool, E. T. *Biochemistry* **1995**, *34*, 4125–4132.
(61) Williams, D. J.; Hall, K. B. *J. Mol. Biol.* **2000**, *297*, 251–265.
(62) Schnizler, K.; Kuster, M.; Methfessel, C.; Fejtl, M. *Receptors Channels* **2003**, *9*, 41–48.
(63) Reardon, P. N.; Spicer, L. D. *J. Am. Chem. Soc.* **2005**, *127*, 10848–10849.
(64) Sakakibara, D.; Sasaki, A.; Ikeya, T.; Hamatsu, J.; Hanashima, T.; Mishima, M.; Yoshimasu, M.; Hayashi, N.; Mikawa, T.; Walchli, M.; Smith, B. O.; Shirakawa, M.; Guntert, P.; Ito, Y. *Nature* **2009**, *458*, 102–105.

processes are still preserved.[16] Whether such a lysate is a good model system, however, has to be evaluated for each project separately.

Acknowledgment. This work was supported by the Grant Agency of AS CR (KAN200100801, Z60220518). Financial support was also obtained from the Center for Biomolecular Magnetic Resonance (BMRZ), the Cluster of Excellence Frankfurt Macromolecular Complexes (CEF) and the Access to Research Infrastructures activity in the sixth Framework Programme of the EC (Contract # RII3-026145, EU-NMR) and are all graciously acknowledged.

Supporting Information Available: Additional experimental data (Figures S1−6). This material is available free of charge via the Internet at http://pubs.acs.org.

JA9052027